Triple Band Reject Frequency Selective Surface with Application to 2.4 GHz Band

Alfrêdo Gomes Neto, Jefferson Costa e Silva, Ianes Barbosa Grécia Coutinho, Marina de Oliveira Alencar, Diego Medeiros de Andrade

***Abstract*— This paper presents the development of a frequency selective surface, FSS, with three bands of rejection, with the central bandwidth applied to the 2.4 GHz frequency band. Despite the fact that the main applications are in the 2.4 GHz frequency band, as emphasized in this paper, to reduce costs with scale production, it is interesting to note when the same FSS can be used for different applications such as wireless and cellular communications (1.71 GHz-1.93 GHz) and radio frequency localization (3.1 GHz-3.3GHz). The three rejection bands are obtained from the association of crossed- dipoles and matryoshka ring geometries. For each geometry the initial design equations are proposed. The procedure to obtain the matryoshka geometry is described step by step. Numerical results are presented for each geometry, and also to the associated geometries, considering different incident angles (θ=0°, 15°, 30° and 45°). The current distribution of each resonant frequency was shown, making it possible to visualize the respective excited geometry. After the numerical results, we verified that the resonant frequencies associated to the respective geometry remained practically unchanged even for the associated geometries. A FSS prototype with the associated geometries was designed, fabricated, and characterized, with a very good agreement between numerical and experimental results, obtaining an attenuation of at least 15 dB in the 2.4 GHz frequency band.**

***Index Terms*— Crossed-dipoles, FSS, Matryoshka, Wi-Fi.**

I. INTRODUCTION

In recent years there has been a large growth in the use of mobile telecommunications services. One of the main drivers of this growth is the massive and diverse development of portable devices, such as smartphones, tablets, laptops, e-book readers, and gaming consoles. This development has provided a true revolution in various areas of human activity, including social interactions, education, health, and commerce. Most of these applications make use of Internet connections, leading to increased demand for transmission rates. Also, services such as video streaming, machine-to-machine (M2M) communication, and Internet of Things (IoT) diversification must be considered, all of which effectively contribute to the growth in demand for higher and higher transmission rates [1], [2].

Considering the limitations of the electromagnetic spectrum, the availability of space for antenna installation, environments with intensive use of wireless communication systems (shopping centers, office buildings, etc.), and sensitive environments (prisons, hospitals, embassies etc.), this means that it is necessary to optimize the use of antennas [3] - [7] as well as to provide solutions to mitigate interference between or limit access to wireless communication systems [8] - [11]. To meet these requirements, one solution is to use frequency selective surfaces (FSS) [12], [13].

Generally speaking, it can be said that a FSS is a periodic arrangement of metallic patch or dielectric slot elements that has the characteristic of reflecting, transmitting or absorbing electromagnetic waves. By allowing or blocking waves in free space, FSS are also called spatial filters [14]-[16]. FSS applications cover a wide range of the electromagnetic spectrum, from microwave to terahertz. These applications include dual-band operating antennas [3], [4], [14], [15], reconfigurable antennas [5], [6], sensors [17], [18], optimization efficiency of communication systems [8] - [11] and energy harvesting [19]. Basically, the frequency response of the FSS is determined by the characteristics of the dielectric, the unit cell geometry, the periodicity of the FSS, and the incident wave polarization, Fig. 1.

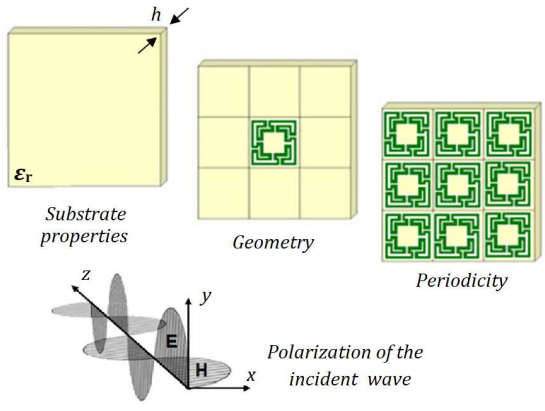

Fig. 1. FSS geometry and parameters that affect the FSS frequency response.

This work was supported in part by the Brazilian National Council of Scientific and Technological Development (Project 407028/2016-1, CNPq), Federal Institute of Paraíba (INTERCONECTA Program-IFPB-PRPIPG 01/2018 and the Postgraduate Program in Electrical Engineering, PPGEE-IFPB).

Alfrêdo Gomes Neto (e-mail: alfredogomesjpa@gmail.com), Jefferson Costa e Silva (e-mail: jefffersoncs@gmail.com), Ianes Barbosa Grécia Coutinho (e-mail: ianesgrecia@gmail.com), Marina de Oliveira Alencar (e-mail: marina.alencar.93@gmail.com), and Diego Medeiros de Andrade (e-mail: diegoandrad96@gmail.com) are with the Group of Telecommunication and Applied Electromagnetism, GTEMA, from the Federal Institute of Paraíba, IFPB.

Digital Object Identifier: 10.14209/jcis.2020.8

One of the challenges in the FSS design is when close resonances are desired, as illustrated in Fig. 2, especially when a single layer FSS is required. [20], [21]. In this case, one of the solutions is to associate different geometries in the composition of the FSS unit cell geometry. To avoid coupling between the different geometries, however, the respective resonances must be due to different field distributions [21].

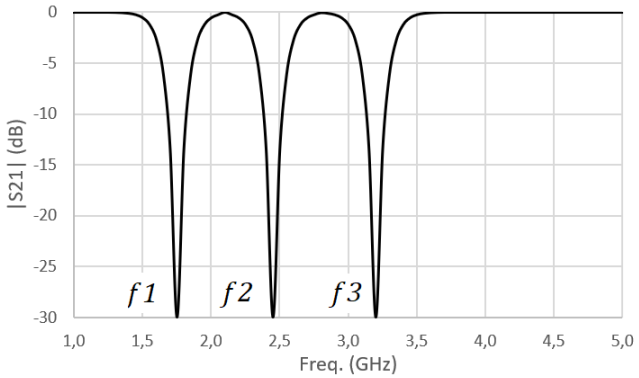

Fig. 2. Frequency response with close resonances.

Recently, matryoshka geometry with characteristics of miniaturization, multiband operation and polarization independence has been described [22], [23]. Taking these characteristics into account, this work presents a FSS with three rejection bands, based on the association of crossed-dipoles and matryoshka geometries. The central rejection band is applied to the Wi-Fi frequency range at 2.4 GHz, being obtained from the crossed-dipoles geometry. The two side rejection bands, 1.8 GHz and 3.2 GHz, are obtained from the resonances of the matryoshka geometry. Despite the fact that the main applications are in the 2.4 GHz frequency band, as emphasized in this paper, to reduce costs for large-scale production, it is interesting to note that the same FSS may be used for different applications, such as wireless and cellular communications (1.71 GHz-1.93 GHz) and radio frequency localization (3.1 GHz-3.3GHz) [24]. The procedure to obtain the matryoshka geometry is described step by step. Initial design equations are proposed for each geometry.

Numerical results are presented considering isolated and associated geometries, for different polarizations and incidence angles ($\theta = 0°, 15°, 30°$ and $45°$). Even with the association of the geometries, the respective resonances were seen to remain unchanged, indicating decoupling between each. In addition to the numerical results, a FSS with the associated geometries was designed, manufactured and characterized experimentally, confirming the expected frequency response, with a very good agreement between the numerical and measured results.

This paper is organized as follows: An introduction is presented in Section I; Section II describes the FSS design steps, showing initial equations for each geometry and the procedure for obtaining the matryoshka ring; in Section III, numerical and experimental results for each geometry and for associated geometries are presented; concluding with Section IV where the results obtained and characteristics achieved are summarized.

II. FSS DESIGN

This section describes the FSS project associating crossed-dipoles and matryoshka geometries. The substrate is considered to have a dielectric constant ε_r and a thickness h.

-Crossed-dipoles geometry

The crossed-dipoles is a very simple geometry, for which the resonant frequency occurs when its length is approximately half of the guided wavelength [14] - [16], Fig. 3.

Determining the dimensions of the FSS basic cell geometry is a process often based on the microwave engineer's experience and usually it is an iterative procedure. From initial dimensions, a numerical optimization is performed until the desired characteristics are achieved. However, equations to establish the initial dimensions can help in the FSS design. In this paper, the following equations are used [25].

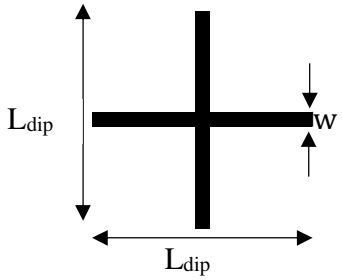

Fig. 3. Crossed-dipoles geometry.

-Dipole length, L_{dip}:

$$L_{dip} = \frac{3\times10^8}{2f_{res}\sqrt{\varepsilon_{ref-dip}}}, \quad (1)$$

in which f_{res} is the desired resonant frequency and $\varepsilon_{ref-dip}$ is given by:

$$\varepsilon_{ref-dip} = \frac{\varepsilon_{ref-MS}+\varepsilon_{ref-CPW}}{2}. \quad (2)$$

Where

ε_{ref-MS} is the effective dielectric constant for a microstrip, considering the microstrip width equal the dipole width, w, and a dielectric thickness h.

$\varepsilon_{ref-CPW}$ is the effective dielectric constant for a coplanar waveguide without ground plane, with $s=10\times h$ and the center strip width equal to the dipole width, w [26].

ε_{ref-MS} and $\varepsilon_{ref-CPW}$ can be easily calculated using available software [27], [28].

-Matryoshka geometry

The matryoshka geometry was introduced in [27], [28]. Differently from concentric rings, in matryoshka geometry the rings are interconnected, as only one ring, increasing its effective length, presenting, consequently, characteristics of miniaturization and multiband operation, Fig. 4. However, this geometry was polarization-dependent. In [22], [23] a polarization independent matryoshka geometry was proposed, Fig. 5, and it is the reference for the geometry considered in this paper. However, in this paper square matryoshka ring was adopted, as it was easier to manufacture than the circular one.

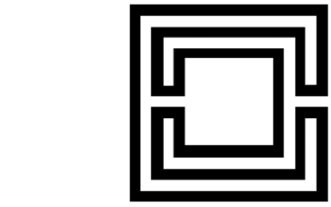

a)Matryohska ring

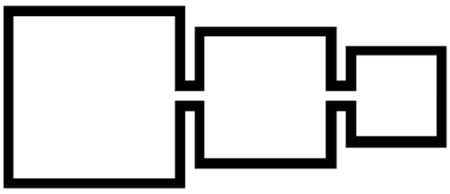

b)Expanded matryohska ring

Fig. 4. Matryoshka geometry.

a)Matryohska circular ring

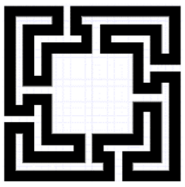

b)Matryohska square ring

Fig. 5. Polarization independent matryoshka geometry.

The matryoshka geometry is obtained by the following steps. Initially, concentric square rings are designed, as depicted in Fig. 6(a). Then, gaps are inserted at the same position in consecutive rings, Fig. 6(b). Finally, the consecutive rings are connected and the matryoshka ring is achieved, Fig. 6(c). Usually, $Lxi = Lyi = Li$, $dxi = dyi = di$, $i = 1,2,3$. The basic cell periodicity is determined by the filling factor, grating lobes limitations, etc. However, in this paper the crossed-dipoles length determined the basic cell periodicity.

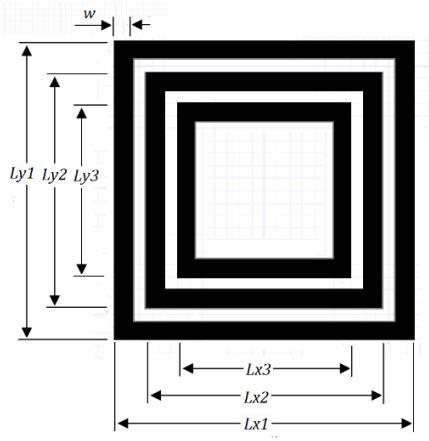

a)Concentric square rings

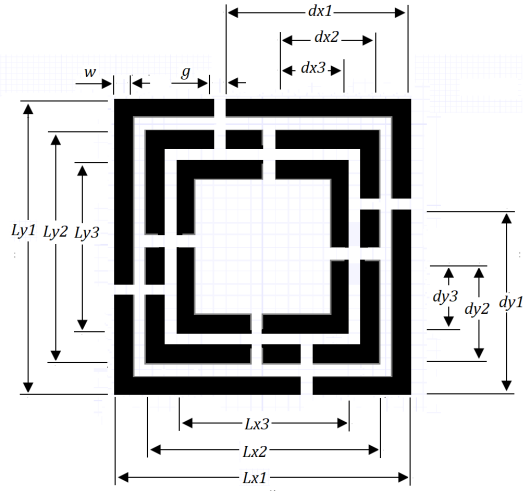

b) Concentric square rings with gaps

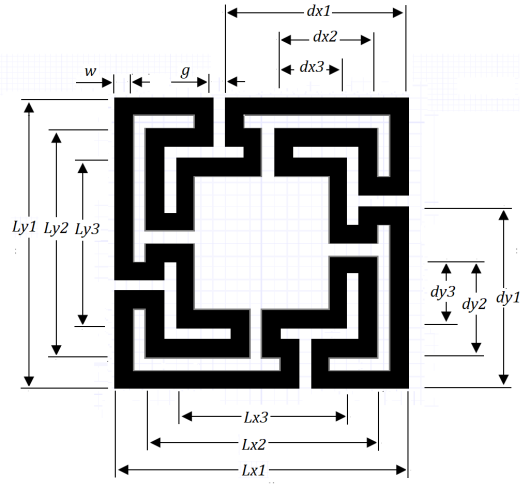

c)Matryoshka square ring geometry

Fig. 6. Polarization independent matryoshka geometry step by step.

Matryoshka geometry presents a multi-resonant behavior [22], [23], [29], [30], but in this paper only the first two resonant frequencies are considered. Analogues to crossed-dipoles geometry, (3)-(6) provide a first approach for the two first resonant frequencies.

-Matryoshka geometry - first resonant frequency:

$$f_{res1} = \frac{3 \times 10^8}{L_{ef1}\sqrt{\varepsilon_{ref-CPW}}}, \quad (3)$$

with

$$L_{ef1} = 3(L_1 - 2w) + 2(L_2 - 2w) + 3(L_3 - 2w) \quad (4)$$

-Matryoshka geometry - second resonant frequency:

$$f_{res2} = \frac{3 \times 10^8}{\left(L_{ef2}/2\right)\sqrt{\varepsilon_{ref-CPW}}}, \quad (5)$$

with

$$L_{ef2} = 3L_1 + 2L_2 + 3L_3 \quad (6)$$

It must be emphasized that (1)–(6) are initial design equations, a first step towards a numerical optimization. Furthermore, the incident wave is considered normal to the FSS ($\theta = 0°$).

Associating the two geometries, the geometry depicted in Fig. 7 is obtained. Note that for ease of visualization, in Fig. 7 (a) the matryoshka geometry was not repeated around the unit cell.

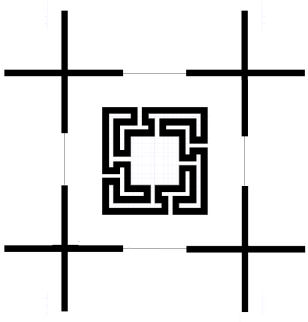

a) Associated geometries

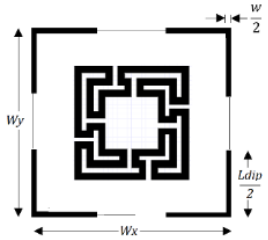

b) FSS basic cell

Fig. 7. FSS basic cell with crossed-dipoles and matryoshka associated geometries.

III. NUMERICAL AND MEASURED RESULTS

Numerical results were obtained using the commercial software ANSYS Designer [31]. The measured results were acquired at the GTEMA/IFPB microwave measurements laboratory using an Agilent E5071C two ports network analyzer, two double ridge horn antennas and a measurement window as shown in Fig. 8. The basic cell dimensions are $40\,mm \times 40\,mm$ ($Wx \times Wy$), and the substrate is a low cost fiber-glass FR-4 ($\varepsilon_r = 4.4$, loss tangent $tg(\delta) = 0.02$, thickness $h = 1.6\,mm$. As the geometry is polarization independent, for numerical results only the x polarization is considered.

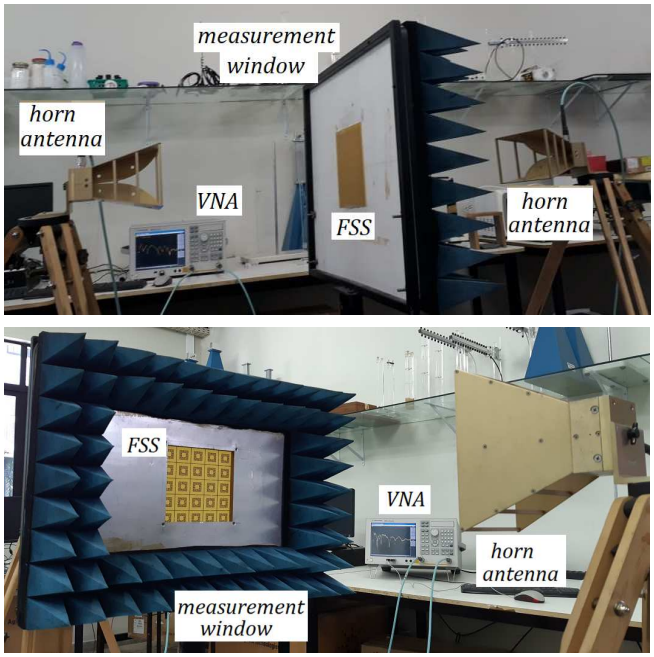

Fig. 8. Measurement setup.

In Fig. 9, the frequency response, $|S21|(dB) \times Freq.(GHz)$, is presented for crossed-dipoles geometry, ($Ldip = 39.0\,mm$, $w = 1.5\,mm$), considering different incidence angles ($\theta = 0°, 15°, 30°$ and $45°$). In the investigated frequency range, from 0.1 GHz to 5.0 GHz, this geometry shows only one resonant frequency, around 2.45 GHz. Practically, the same frequency response is observed for the different incidence angles. The incipient resonances at 3.17 GHz ($\theta \neq 0°$) are due to the grating lobes. For $\theta = 0°$, the resonant frequency calculated by (1), and the measured one, present almost the same value, 2.45 GHz. The Table I summarizes the results, in which we can observe a very good angular stability.

In a similar way, Fig. 10 shows the frequency responses for the matryoshka geometry, with $w = 1.5\,mm$, $g = 1.0\,mm$, $L1 = 24.0\,mm$, $L2 = 1.0\,mm$, $L3 = 14.0\,mm$, $d1 = 15.0\,mm$, $d2 = 8.5\,mm$, $d3 = 6.0\,mm$. The first two resonant frequencies are approximately the same for the considered incidence angles, 1.81 GHz and 3.16 GHz. For $\theta = 0°$, the resonant frequencies calculated by (3)-(6), are 1.94 GHz and

3.27 GHz, a difference of 6.4% and 2.9%, respectively. When compared to numerical results, this is a good approximation for a first approach. Also noteworthy is a reduction in the first resonant frequency of 25.6%, from 2.46 GHz to 1.81 GHz, when comparing crossed-dipoles and matryoshka geometries, even though the crossed-dipoles are 62.5% larger than matryoshka, 39.0 mm and 24.0 mm, respectively. Table II summarizes the results, in which very good angular stability is observed again.

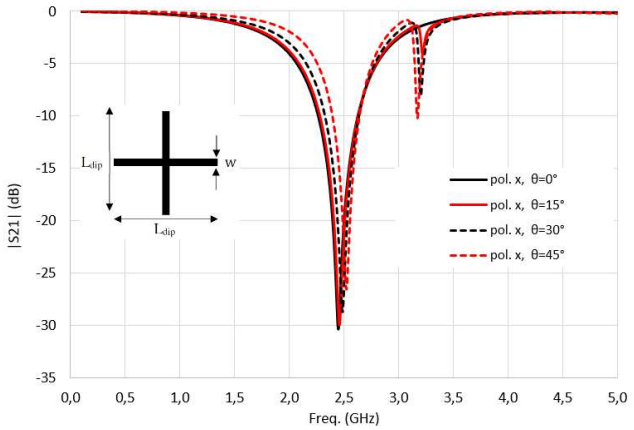

Fig. 9. Frequency response, crossed-dipoles, $Ldip = 39\ mm$, $w = 1.5\ mm$.

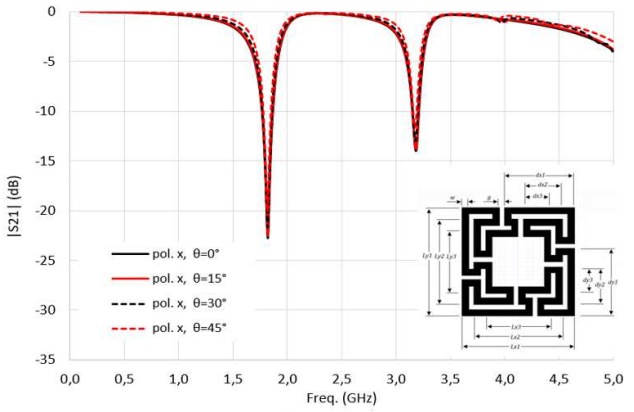

Fig. 10. Frequency response, matryoshka, $w = 1.5\ mm, g = 1.0\ mm, L1 = 24.0\ mm, L2 = 1.0\ mm, L3 = 14.0\ mm, d1 = 15.0\ mm, d2 = 8.5\ mm, d3 = 6.0\ mm$.

TABLE I - RESONANT FREQUENCIES FOR DIFFERENT INCIDENCE ANGLES – CROSSED-DIPOLES GEOMETRY.

	$\theta = 0°$	$\theta = 15°$	$\theta = 30°$	$\theta = 45°$
$f_{res.}$ (Num.)	2.445 GHz	2.455 GHz	2.485 GHz	2.520 GHz
$f_{res.}$ (1)	2.453 GHz	2.453 GHz	2.453 GHz	2.453 GHz
Difference	-0.33%	0.08%	1.30%	2.73%

TABLE II - RESONANT FREQUENCIES FOR DIFFERENT INCIDENCE ANGLES – MATRYOSHKA GEOMETRY.

	$\theta = 0°$	$\theta = 15°$	$\theta = 30°$	$\theta = 45°$
$f_{res1.}$ (Num.)	1.815 GHz	1.815 GHz	1.820 GHz	1.820 GHz
$f_{res1.}$ (3),(4)	1.940 GHz	1.940 GHz	1.940 GHz	1.940 GHz
Difference	-6.44%	-6.44%	-6.18%	-6.18%
$f_{res2.}$ (Num.)	3.180 GHz	3.180 GHz	3.180 GHz	3.175 GHz
$f_{res2.}$ (5),(6)	3.270 GHz	3.270 GHz	3.270 GHz	3.270 GHz
Difference	-2.75%	-2.75%	-2.75%	-2.91%

The frequency response for the two associated geometries is presented in Fig. 11. Three resonant frequencies are observed, 1.81 GHz, 2.44 GHz and 3.18 GHz, with the first and third resonances being associated with the matryoshka geometry and the second one with the crossed-dipoles. It is also verified that these resonance frequencies practically did not shift in relation to the values of the isolated geometries. Even the grating lobes (around 3.1 GHz) are present in the frequency response for $\theta \neq 0°$. In Fig. 12 the current distribution is displayed for each resonant frequency and the geometry that produces this resonance can be identified. In Figs. 12(a) and 12(c), 1.81 GHz and 3.18 GHz, respectively, only the matryoshka is excited, and in Fig. 12(b), 2.43 GHz the crossed-dipoles are excited.

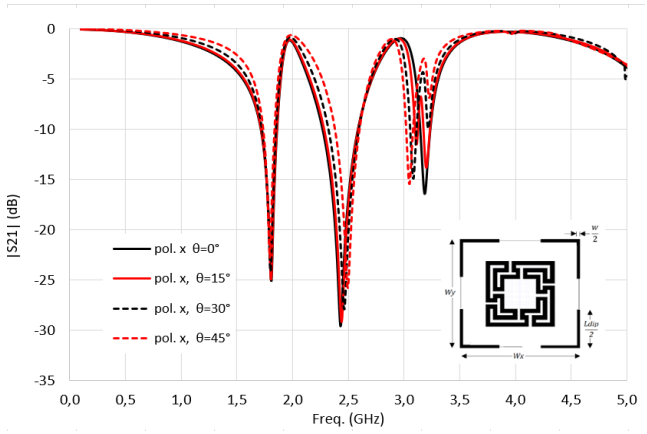

Fig.11. Frequency response, crossed-dipoles and matryoshka associated geometries.

In order to verify experimentally the frequency response behavior for the associated geometries, a FSS prototype was designed, fabricated and characterized. The dimensions and materials are the same previously described, Fig. 10. The whole FSS has 5×5 basic cells, corresponding to $20\ cm \times 20\ cm$, Fig. 13. Measured results for crossed-dipoles and matryoshka associated geometries are presented in Fig. 14, normal incidence $\theta = 0°$, considering x and y polarizations. When compared to numerical results, a very good agreement is verified and an attenuation of at least 15 dB is achieved in the

Wi-Fi band (2.4 GHz). Moreover, the polarization independence is confirmed. The results are show in Table III.

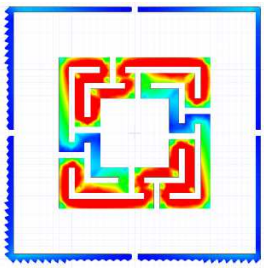

a)Current distribution, freq. = 1.81 GHz

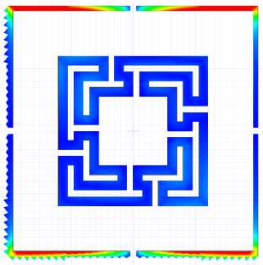

b)Current distribution, freq. = 2.43 GHz

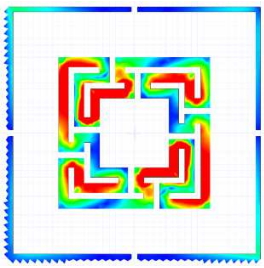

c)Current distribution, freq. = 3.18 GHz

Fig.12. Current distribution for different resonant frequencies.

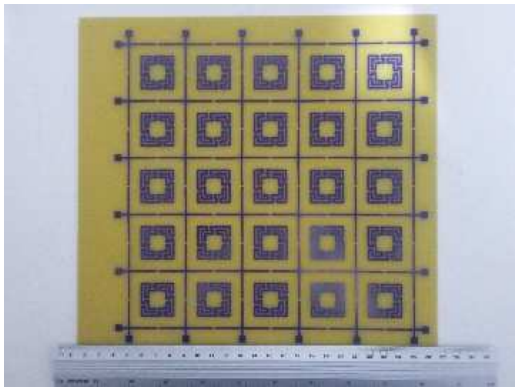

Fig. 13. FSS prototype.

In Figs. 15, 16 and 17, the measured results are presented for x polarization, considering $\theta = 15°, 30°, 45°$, respectively. In Table IV, the resonant frequencies are summarized, including $\theta = 0°$. A first point to be highlighted is the good agreement between numerical and measured resonant frequencies. Furthermore, the angular stability is verified. For $\theta = 30°, 45°$, a greater difference between the results is observed, especially for higher frequencies, but this is due to the absorbers in the measurement window that blocked the incident wave.

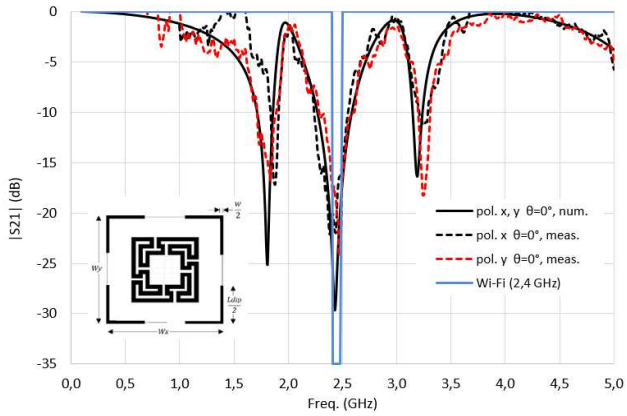

Fig. 14. Frequency response, crossed-dipoles and matryoshka associated geometries, measured results, normal incidence $\theta = 0°$.

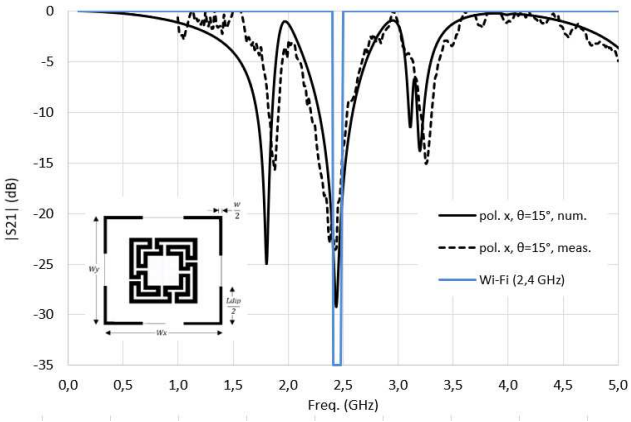

Fig. 15. Frequency response, crossed-dipoles and matryoshka associated geometries, measured results, $\theta = 15°$, pol. x.

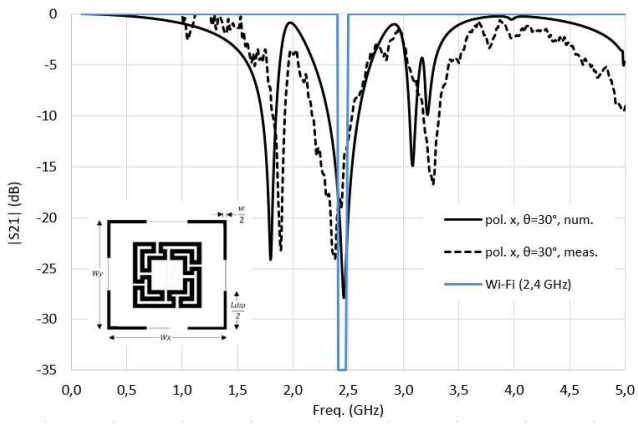

Fig. 16. Frequency response, crossed-dipoles and matryoshka associated geometries, measured results, $\theta = 30°$, pol. x.

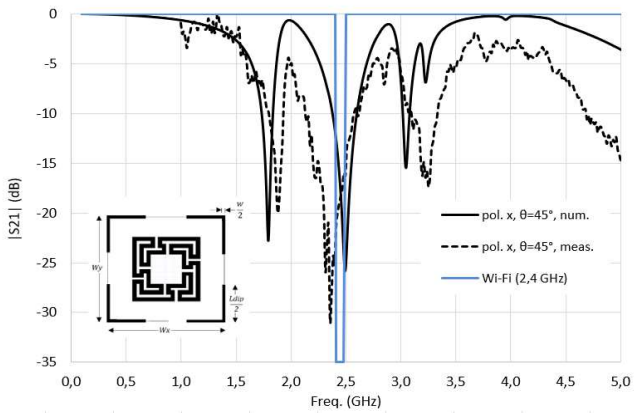

Fig. 17. Frequency response, crossed-dipoles and matryoshka associated geometries, measured results, $\theta = 45°$, pol. *x*.

TABLE III - RESONANT FREQUENCIES FOR NORMAL INCIDENCE, $\theta = 0°$ CROSSED-DIPOLES AND MATRYOSHKA ASSOCIATED GEOMETRIES.

	pol. x	***pol. y***
$f_{res1.}$ (Num.)	1.815 GHz	1.815 GHz
$f_{res1.}$ (meas.)	1.882 GHz	1.835 GHz
Difference	-3.56%	-1.09%
$f_{res2.}$ (Num.)	2.430 GHz	2.430 GHz
$f_{res2.}$ (meas.)	2.386 GHz	2.467 GHz
Difference	1.84%	-1.50%
$f_{res3.}$ (Num.)	3.190 GHz	3.190 GHz
$f_{res3.}$ (meas.)	3.254 GHz	3.239 GHz
Difference	-1.97%	-1.51%

TABLE IV - RESONANT FREQUENCIES FOR $\theta = 0°, 15°, 30°, 45°$, CROSSED-DIPOLES AND MATRYOSHKA ASSOCIATED GEOMETRIES, POL. *X*.

	$\boldsymbol{\theta = 0°}$	$\boldsymbol{\theta = 15°}$	$\boldsymbol{\theta = 30°}$	$\boldsymbol{\theta = 45°}$
$f_{res1.}$ (Num.)	1.815 GHz	1.805 GHz	1.800 GHz	1.795 GHz
$f_{res1.}$ (Meas.)	1.882 GHz	1.882 GHz	1.896 GHz	1.882 GHz
Difference	-3.56%	-4.09%	-5.06%	-4.62%
$f_{res2.}$ (Num.)	2.430 GHz	2.440 GHz	2.465 GHz	2.495 GHz
$f_{res2.}$ (Meas.)	2.386 GHz	2.428 GHz	2.386 GHz	2.400 GHz
Difference	1.84%	0.49%	3.31%	3.96%
$f_{res3.}$ (Num.)	3.190 GHz	3.200 GHz	3.085 GHz	3.050 GHz
$f_{res3.}$ (Meas.)	3.254 GHz	3.254 GHz	3.268 GHz	3.254 GHz
Difference	-1.97%	-1.66%	-5.60%	-6.27%

IV. CONCLUSIONS

In this paper, a triple band reject FSS with application to 2.4 GHz band is described. The proposed FSS is single layer and based on the association of two distinct geometries: crossed-dipoles and matryoshka. The main idea when using distinct geometries is to avoid the coupling between them, keeping the features of each geometry in the associated geometries.

For each geometry, the initial design equations were proposed and verified by numerical simulations, achieving a good agreement. The individual geometries were numerically characterized for different incidence angles. Similarly, FSS with associated geometries was numerically characterized, confirming the expected frequency response, with the resonant frequencies of each geometry maintaining practically the same. The current distribution of each resonant frequency was shown, allowing to visualize the respective excited geometry.

A FSS prototype was designed, fabricated and numerically and experimentally characterized, considering incidence angles of 0°, 15°, 30° and 45°. The obtained results confirm the expected frequency response, including the polarization independence and angular stability, and indicating the decoupling between the associated geometries. In this way, the triple-band FSS was successfully reached, obtaining an attenuation of at least 15 dB in the 2.4 GHz frequency band.

REFERENCES

[1] Cisco Visual Networking, "Global Mobile Data Traffic Forecast Update 2017–2022" https://www.cisco.com/c/en/us/solutions/collateral/service-provider/visual-networking-index-vni/white-paper-c11-738429.html. [Acesso em 6 de março 2019]

[2] Ibraheem Shayea, Marwan Hadri Azmi, Tharek Abd. Rahman, Mustafa Ergen, Chua Tien Han, and Arsany Arsad, "Spectrum gap analysis with practical solutions for future mobile data traffic growth in Malaysia," *IEEE Access*, 24910-24933, Mar. 2019. doi: 10.1109/ACCESS.2018.2890302.

[3] Tiago Henrique Brandão, Antenas Parabólicas de Banda Dupla Baseadas em FSS para Radares e Comunicação, *in Portuguese*, Master thesis, INATEL, Santa Rita do Sapucaí, MG, Brazil, 2019.

[4] T.H. Brandão, H. R. D. Filgueiras, Juliano F. Mologni, Antonella Bogoni and Arismar Cerqueira S. Jr., "FSS-based dual-band Cassegrain Parabolic antenna for radarcomm applications," *2017 SBMO/IEEE MTT-S International Microwave and Optoelectronics Conference (IMOC)*, Águas de Lindóia, SP, 2017, pp. 1-5. doi: 10.1109/IMOC.2017.8121131.

[5] M. Bouslama, M. Traii, T. A. Denidni, and A. Gharsallah, "Beam-switching antenna with a new reconfigurable frequency selective surface," *IEEE Antennas Wireless Propag. Lett.*, vol. 15, pp. 1159–1162, 2016. doi: 10.1109/LAWP.2015.2497357.

[6] João R. Reis, Akram Hammoudeh, Nigel Copner, Telmo Fernandes, Rafael F. S. Caldeirinha, "2D Agile beamsteering using an electronically reconfigurable transmitarray," *13th European Conference on Antennas and Propagation (EuCAP 2019)*, Krakow, Poland, Mar. 31-Apr. 5, 2019, pp. 1-5.

[7] A. Kesavan, M. Mantash, J. Zaid and T. A. Denidni, "A dual-plane beam-sweeping millimeter-wave antenna using reconfigurable frequency selective surfaces," in *IEEE Antennas and Wireless Propagation Letters*, vol. 17, no. 10, pp. 1832-1836, Oct. 2018. doi: 10.1109/LAWP.2018.2867331

[8] S. Cho, I. Lee and I. Hong, "Frequency selective film design for building walls for blocking wireless lan signal," *2018 International Symposium on Antennas and Propagation (ISAP)*, Busan, Korea (South), 2018, pp. 1-2.

[9] S. Habib, G. I. Kiani, and M. F. U. Butt, "Interference mitigation and WLAN efficiency in modern buildings using energy saving techniques and FSS," in *2016 IEEE International Symposium on Antennas and*

Propagation (APSURSI), Fajardo, Puerto Rico, July, 1, 2016, pp. 965–966. doi: 10.1109/APS.2016.7696191.

[10] G. I. Kiani and R. W. Aldhaheri, "Wide band FSS for increased thermal and communication efficiency in smart buildings," *2014 IEEE Antennas and Propagation Society International Symposium (APSURSI)*, Memphis, TN, 2014, pp. 2064-2065. doi: 10.1109/APS.2014.6905359

[11] C. J. Davenport, J. M. Rigelsford, J. Zhang and H. Altan, "Periodic comb reflection frequency selective surface for interference reduction," *2013 Loughborough Antennas & Propagation Conference (LAPC)*, Loughborough, 2013, pp. 615-618. doi: 10.1109/LAPC.2013.6711974.

[12] Ravi Panwar, Jung Ryul Lee, "Progress in frequency selective surface-based smart electromagnetic structures: Acritical review," *Aerospace Science and Technology*, (66), pp. 216–234, 2017. doi.org/10.1016/j.ast.2017.03.006.

[13] Rana Sadaf Anwar, Lingfeng Mao and Huansheng Ning, "Frequency Selective Surfaces: A Review," *Applied Sciences*, vol. 8, no. 9: 1689, Sep. 2018. doi:.org/10.3390/app8091689.

[14] John C. Vardaxoglou, Frequency Selective Surfaces – Analysis and Design, Research Studies Press, England, 1997.

[15] B. A. Munk, Frequency Selective Surfaces - Theory and Design, New York: Wiley, 2000.

[16] A. L. P. S. Campos, Superfícies Seletivas em Frequência – Análise e Projeto, *in Portuguese*, IFRN Editora, Natal, Brazil, 2009.

[17] M. Mahmoodi and K. M. Donnell, "Active frequency selective surface for strain sensing," in *2017 IEEE International Symposium on Antennas and Propagation & USNC/URSI National Radio Science Meeting*, San Diego, California, USA, July 2017, pp. 675–676. doi: 10.1109/APUSNCURSINRSM.2017.8072380.

[18] S. Milici, A. Lazaro, J. Lorenzo, R. Villarino, D. Girbau, "Wearable sensors based on modulated frequency selective surfaces," in *47th European Microwave Conference (EuMC)*, Nuremberg, 2017, pp. 942-945. doi: 10.23919/EuMC.2017.8231001.

[19] F. Erkmen, T. S. Almoneef and O. M. Ramahi, "Scalable electromagnetic energy harvesting using frequency selective surfaces," in *IEEE Transactions on Microwave Theory and Techniques*, vol. 66, no. 5, pp. 2433-2441, May 2018. doi: 10.1109/TMTT.2018.2804956.

[20] S. Genovesi, F. Costa and A. Monorchio, "Design of compact multiband frequency selective surfaces with meandered elements," *2017 47th European Microwave Conference (EuMC)*, Nuremberg, 2017, pp. 604-607. doi: 10.23919/EuMC.2017.8230920.

[21] A. G. Neto, J. C. e. Silva, J. B. d. O. Silva and C. Peixeiro, "A dual-band frequency selective surface using four arms star geometry associated to trapezoidal rings for WiFi applications," *2017 47th European Microwave Conference (EuMC)*, Nuremberg, 2017, pp. 791-794. doi: 10.23919/EuMC.2017.8230966.

[22] A. G. Neto, T. R. de Sousa, J. C. E. Silva and D. F. Mamedes, "A polarization independent frequency selective surface based on the matryoshka geometry," *2018 IEEE/MTT-S International Microwave Symposium - IMS*, Philadelphia, PA, 2018, pp. 999-1002. doi: 10.1109/MWSYM.2018.8439231.

[23] Thayuan Rolim de Sousa, Desenvolvimento de Superfícies Seletivas em Frequência Baseadas na Geometria Matrioska Independente da Polarização, *in Portuguese*, Master thesis, PPGEE, IFPB, João Pessoa, PB, Brasil, 2019.

[24] ANATEL, Plano de Atribuição, Destinação e Distribuição de Frequências no Brasil, *in Portuguese*, Brasília, Brasil, 2020.

[25] Ianes Barbosa Grécia Coutinho, Desenvolvimento de Superfícies Seletivas em Frequência Associando as Geometrias Dipolos Cruzados e Matrioska, *in Portuguese*, Master thesis, PPGEE, IFPB, João Pessoa, PB, Brasil, 2020.

[26] R. Simons, *Coplanar Waveguide Circuits, Components, and Systems*, USA: Wiley, 2001.

[27] http://www.hp.woodshot.com.

[28] https://www.emtalk.com/mscalc.php

[29] Hillner de Paiva Almeida Ferreira, Uma Proposta de Geometria para FSS Multibandas, *in Portuguese*, Master thesis, PPGEE, IFPB, João Pessoa, PB, Brazil, 2014.

[30] A. Gomes Neto, A. G. DAssunção, J. C. e. Silva, A. N. d. Silva, H. d. P. A. Ferreira and I. S. S. Lima, "A proposed geometry for multi-resonant frequency selective surfaces," *2014 44th European Microwave Conference*, Rome, 2014, pp. 897-900. doi: 10.1109/EuMC.2014.6986580.

[31] http://www.ansys.com.

Alfredo Gomes Neto received the B.Sc. degree from Federal University of Paraíba, Campina Grande, PB, Brazil, 1986, M.Sc., 1989, and D.Sc., 1994, all in electrical engineering and in microwave area, from the same University. In 1993, he held part of his D.Sc. at the ENSEEIHT, INPT, Toulouse, France, to where he returned in 2005, during the post-doctorate researches. Since 1989 he is with the Federal Institute of Paraíba, IFPB. In 1994 he was a founder of the Group of Telecommunications and Applied Electromagnetism, GTEMA, at the IFPB. He is a member of the Brazilian Society of Microwaves and Optoelectronics, SBMO, and IEEE Senior Member. His research interests include electromagnetic theory, microwaves, wave propagation, FSS, antennas and numerical methods.

Jefferson C. Silva received the B.Sc. and M.Sc. degrees in electrical engineering from the Federal University of Paraíba, PB, Brazil, in 1990 and 1993, respectively, and the Ph.D. degree in electrical engineering from Federal University of Rio Grande do Norte, Natal, RN, Brazil in 2005. From 1992 to 1993, he was Assistant Professor at the Federal University of Maranhão, MA, Brazil. Since 1993, he has been with the Industry Academic Unit, Federal Institute of Paraíba, PB, Brazil, where he is Full Professor. He is the author of two book chapters, more than 70 articles, and 5 patent registers. His research interests include antennas and propagation, applied electromagnetism, antennas and propagation measurements and numeric simulations. He is IEEE member since 2012.

Ianes Barbosa Grécia Coutinho received the B. Sc. and M.Sc. degree in electrical engineering (telecommunications) from the Federal Institute of Paraiba (IFPB), Brazil, in 2018 and 2020, respectively. He is currently pursuing his D.Sc. degree in electrical engineering at the Federal University of Campina Grande (UFCG), PB, Brazil. His research interests include microstrips antennas, sensors and frequency selective surface.

Marina de Oliveira Alencar received the B.Sc. and M.Sc. degrees in electrical engineering (telecommunications) from the Federal Institute of Paraíba (IFPB), PB, Brazil, in 2018, and 2020, respectively. Her research interests are applied electromagnetism, frequency selective surfaces (FSS) and antennas.

Diego Medeiros de Andrade is currently working toward the B.Sc. degree in electrical engineering at the Federal Institute of Paraíba (IFPB), PB, Brazil. His research interests include frequency selective surfaces (FSS) and antennas.